

NANO EXPRESS

Open Access



ESR Study of (La,Ba)MnO₃/ZnO Nanostructure for Resistive Switching Device

Taras Polek^{1*}, Mykhaylo Semen'ko², Tamio Endo³, Yoshinobu Nakamura⁴, Gurmeet Singh Lotey⁵ and Alexandr Tovstolytkin¹

Abstract

Structure, electric, and resonance properties of (La,Ba)MnO₃/ZnO nanostructure grown on SrTiO₃ (001) substrate have been investigated. It is found that at room temperature and relatively low voltages ($|V| < 0.2$ V), the structure shows good rectification behavior with rectification factor near 210. Resistive switching properties are detected after application of higher voltages. Temperature evolution of magnetic phase composition of the sample is analyzed in detail, based on results of electron spin resonance measurements. It is shown that magnetic state below 260 K is characterized by coexistence of ferromagnetic and paramagnetic phases, but no evidence of magnetic phase separation is revealed at higher temperatures. Different driving mechanisms for resistive switching, such as magnetic phase separation and/or electric field-induced migration of oxygen vacancies, are discussed in the context of obtained results.

Keywords: Substituted manganites, Oxide nanostructures, *p-n* heterojunctions, Rectification factor, Resistive switching, Electron spin resonance, Magnetic phase separation

PACS: 75.47.m, 73.40.Ei, 75.75.a, 76.50.g, 75.30.m

Background

Oxides of transition metals offer an attractive platform for new applications in electronics, spintronics, and optoelectronics. Complex oxides with perovskite structure occupy a special place among all oxide materials, since they display a rich variety of fascinating properties such as high-temperature superconductivity [1], colossal magnetoresistance (CMR) [2], left-handed properties [3, 4], and others. A peculiar feature of the CMR materials, to which belong manganese-based perovskites such as La_{1-x}Me_xMnO₃ (Me = Ba, Sr, Ca...), is that paramagnetic to ferromagnetic transition is accompanied by a transition from *p*-type semiconducting to metallic conductivity [2, 5]. Due to a number of competitive interactions, the ground state of bulk and thin films of La_{1-x}Me_xMnO₃ is often phase separated and usually characterized by a coexistence

of highly conductive ferromagnetic (FM) phase and poorly conductive paramagnetic (PM) or charge-ordered phases [2]. Such complexity of the properties of perovskite manganites has become the point of attraction for a vast number of researchers around the world [2, 5, 6]. It is expected that this class of materials will create the foundation for various applications, such as low-field magnetoresistance sensors, resistive switching devices, and others [6, 7].

On the other hand, ZnO is a typical *n*-type semiconductor with a 3.4-eV band gap [8, 9]. This material is transparent for a visible spectrum but absorbs ultraviolet. There have been reports about ultraviolet stimulated emission and lasing from ZnO thin films [8]. The oxide is also promising for such applications as sensors and organic solar cells [9–11].

Thin films of oxides, such as ZnO, La_{1-x}Ba_xMnO₃ (LBMO), La_{1-x}Sr_xMnO₃ (LSMO), Nd-doped SrTiO₃, and others, often display resistive switching properties, i.e., sharp change of resistivity under electric field or current, and are promising for the use in non-volatile memory

* Correspondence: polek.taras@gmail.com

¹Institute of Magnetism, 36b Vernadsky Boulevard, Kyiv 03680, Ukraine
Full list of author information is available at the end of the article

elements [12]. To date, there has been no unique explanation of this phenomenon, although some models for the driving mechanisms of resistive switching have been proposed. The authors of [13] concluded that formation of a conducting path within a dielectric layer is responsible for the phenomenon in a metal/binary oxide/metal sandwich. They succeeded in direct observation of the inhomogeneous spatial structure of the conducting path, which was formed upon the initial voltage application. A thermal or electrochemical redox reaction in the vicinity of the interface between the oxide and the metal electrode was suggested as other plausible mechanism for resistive switching [14]. It was concluded, however, that further research from chemical, electronic, and crystallographic viewpoints is needed to elucidate actual microscopic mechanism because the chemical, electronic, and crystallographic properties of the oxides, as well as the metal electrodes, affect the mechanism.

A great deal of efforts has been concentrated on fabrication and investigation of oxide-based *p-n* heterojunctions. Zhang et al. [15] found that the *p-n* junction formed from ZnO nanosheet on LSMO thin film showed a high rectification factor of 120 at room temperature. Khachar et al. [16] reported magnetic field modulations of current–voltage (*I-V*) characteristics for ZnO/(La,Pr,Sr)MnO₃/(Sr,Nb)TiO₃-substrate system. The rectification factor was not very high, but the current was field sensitive at 300 K. The authors suggested that the modification of the rectifying behavior can be ascribed to the interface effects due to the change of the crystal field splitting of manganese *d* levels. The optical and magnetic field induced transformations of current–voltage characteristics of ZnO/LSMO nanostructure grown on LaAlO₃ substrate were studied in Ref. [17]. It was suggested that the shape and size of the energy barrier were changed by the modifications of junction interface and interface tensile strain due to optical and magnetic external perturbations.

The attempts to tune resistive, rectifying, and magnetic properties of zinc oxide/substituted manganite nanostructures have been made by the authors of Refs. [17–21], who, in particular, studied the effects of temperature and magnetic field [18], changes in thickness of ZnO [14] and manganite [19] layers, effects of substrate kind and white light irradiation [20], etc.

Okada et al. [22] fabricated and investigated ZnO/substituted manganite bilayers on different substrates. They reported rectification properties and resistive switching over a wide temperature range. It was suggested that the driving mechanism for resistive switching is a coexistence of highly conductive FM phase and poorly conducting charge-ordered or PM phase in manganite layer. Taking into account that the existence of mixed magnetic/conductive state is a characteristic feature of substituted

manganites [23, 24], further investigations are needed to examine the magnetic state of such structures and, thus, prove or disprove the above suggestion. One of the most efficient methods suitable for this aim is electron spin resonance (ESR), which makes it possible to separately analyze the parameters of different coexisting magnetic phases. This work is aimed at investigation of ESR properties of LBMO/ZnO nanostructure grown on SrTiO₃ (STO) substrate and elucidation of the driving mechanism for the resistive switching properties.

Methods

The LBMO/ZnO nanostructure was fabricated on SrTiO₃ (001) substrate by ion-beam sputtering from (La,Ba)MnO₃ and ZnO targets, as described in Ref. [22]. The deposition was performed with ultralow deposition rate (near 10⁻³ nm/s) in two stages: at first, ZnO underlayer was grown on SrTiO₃ (001) substrate at 400 °C, and then secondary LBMO overlayer was deposited on the ZnO underlayer at 600 °C. The layer thickness, estimated as a product of deposition time and deposition rate, was around 100 nm for each of two layers.

The sample was characterized by the X-ray DRON-4 diffractometer using CoK α radiation. X-ray data were separately collected from both the bilayer and substrate sides.

Current–voltage characteristics were measured using a standard four-point probe method. Indium electrodes were placed on the surface of LBMO/ZnO bilayer having the step-shape, two electrodes on the surface of each layer. Ohmic behavior of the contacts was proved based on the observation of linear current–voltage characteristics for each pair of electrodes (placed either on LBMO or on ZnO layer).

ESR studies were carried out in the temperature range 100–300 K with the use of ELEXSYS E500 spectrometer equipped with an automatic goniometer. The operating frequency was $f = 9.47$ GHz. The temperature dependences of the ESR spectra were studied in two geometry configurations: external magnetic field is perpendicular and parallel to the film plane ($\theta = 0^\circ$ and 90° , respectively, where θ is an angle between external magnetic field **H** and film normal). In addition, the out-of-plane angle dependences of the resonance fields, $H_{\text{res}}(\theta, T = \text{const})$, were investigated at selected temperatures.

Results and Discussion

X-ray diffraction patterns, obtained by the collection of the data from the substrate side, contain only STO (001), (002), (003), and (004) reflections. The lattice parameter determined from the positions of (003) and (004) reflections is $a = 0.39069(18)$ nm, which is close to the data of Ref. [25] ($a = 0.39050$ nm). The diffractogram, taken from the bilayer side, shows LBMO (110) peak and ZnO (002), (110), and (004) peaks in addition to the

STO substrate peaks (Fig. 1). The main orientation of ZnO is (001), and LBMO has single phase of (110).

The LBMO/ZnO nanostructure shows fine rectification behavior at room temperature (295 K), and for relatively low voltage ($|V| < 0.2$ V), the I – V characteristics are fully reversible. Under these conditions, rectification factor is near 210.

To prove the reversibility of the low-voltage I – V characteristics, 4 sets of measurements at regular intervals (4 days) were carried out. Each set included 25 measurement cycles with $|V| < 0.2$ V. Inset of Fig. 2 compares the first and hundredth I – V characteristics. It is seen that the difference is negligible.

Quite different behavior is observed after application of higher voltages. Figure 2 shows evolution of current–voltage characteristics of the LBMO/ZnO sample as the number of I – V measurement cycles increases. The duration of one measurement cycle was 2 min. Each subsequent measurement cycle was carried out in 10 min after the previous one. The original I – V curve is characteristic of a typical p – n junction. However, after running the first measurement cycle, the I – V dependence shows a clear one-step switching near 3 V in the forward and a clear two-step switching around -0.2 and -2.0 V in the reverse bias. In addition, it shows a very low resistance near zero Volts in the reverse side. Thus, the sample shows the transition from the very low resistant state, to the intermediate resistant state, and finally to the high resistant state with increasing the reverse voltage [22]. Further, after running the second measurement cycle, the I – V dependence shows a kink near 4 V in the forward (disappearance of one-step switching) and the one-step switching in the reverse bias (disappearance of two-step switching). On the whole, the forward current decreases while the reverse current increases with increasing the number of measurement cycles.

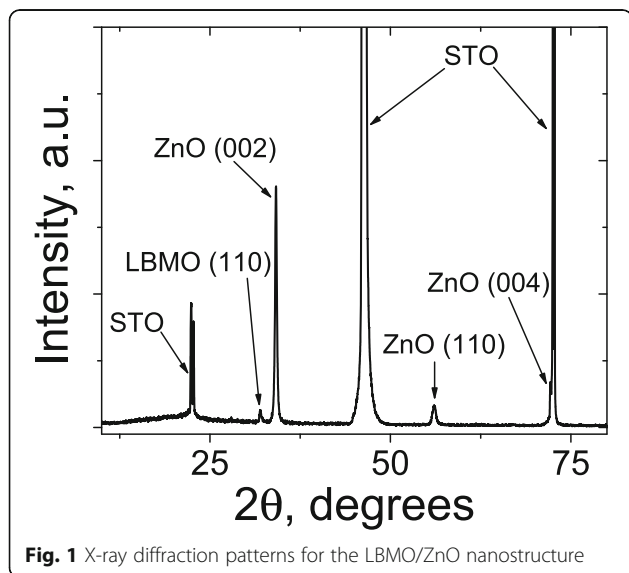


Fig. 1 X-ray diffraction patterns for the LBMO/ZnO nanostructure

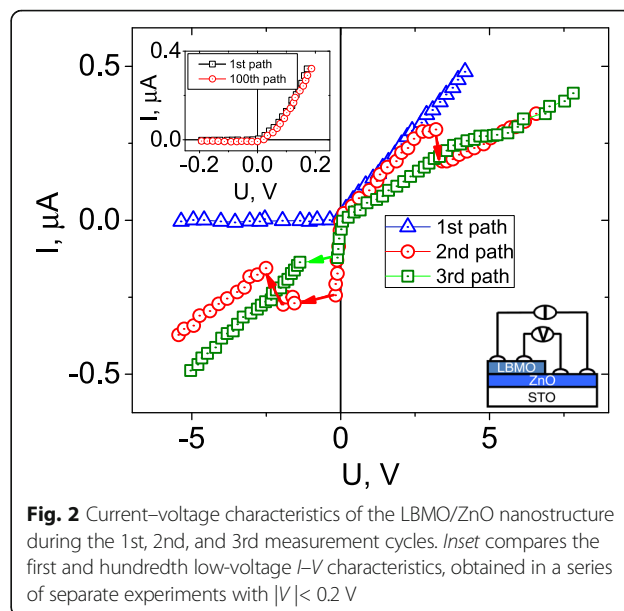
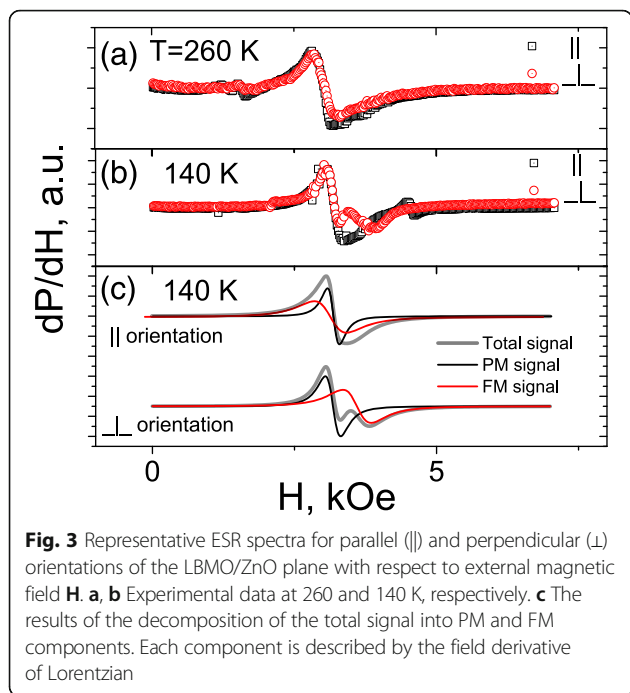


Fig. 2 Current–voltage characteristics of the LBMO/ZnO nanostructure during the 1st, 2nd, and 3rd measurement cycles. *Inset* compares the first and hundredth low-voltage I – V characteristics, obtained in a series of separate experiments with $|V| < 0.2$ V

This implies that the change of electric state is not caused by sample degradation. It is noteworthy that the original rectification behavior is usually resumed after a few days, indicating that high-voltage-induced state is metastable.

To study the temperature evolution of the LBMO magnetic phase composition, ESR measurements were carried out in the temperature range from 120 to 300 K. Two geometric configurations were chosen for measurements: external magnetic field \mathbf{H} was either perpendicular (\perp) or parallel (\parallel) to the film plane. Such measurement procedure makes it possible to separate the signals originated from FM and other magnetic phases, if they are present in the sample [26].

Representative ESR spectra for 260 and 140 K are shown in Fig. 3. At 260 K, the spectrum consists of one resonance signal whose parameters (position on the field scale and linewidth) are insensitive to the sample orientation (within the measurement error). The resonance field ($H_{\text{res}} \approx 3120$ Oe) corresponds to Lande g -factor approximately equal 2, which is a characteristic of PM state of substituted manganites [23]. At the same time, at 140 K, more complicated behavior is observed. Comparison of the spectra for perpendicular and parallel measurement geometries makes it possible to conclude that the spectrum consists of two resonance signals. The first one with resonance field $H_{\text{res1}} \approx 3230$ Oe is the signal from PM phase. Its position on the field scale does not depend on the sample orientation. The position of the second signal is sensitive to the orientation of the sample with respect to the external magnetic field. For perpendicular orientation, this signal has resonance field $H_{\text{res2}}^{\perp} \approx 3690$ Oe, and it is well discernible in the total



spectrum. Such behavior is a characteristic of the signal originated from FM phase [23, 27].

Very narrow weak signals, observed in all spectra under discussion, originate from paramagnetic impurities in the substrate [24], and they are not analyzed in this work.

Magnetic resonance in FM state is governed by the effective magnetization, and this depends on the spontaneous magnetization as well as anisotropies due to shape, strain, and crystallinity. For isotropic thin films, in which we assume anisotropy only due to shape, the resonance may be described using the Kittel's equations with appropriate demagnetizing factors [27]:

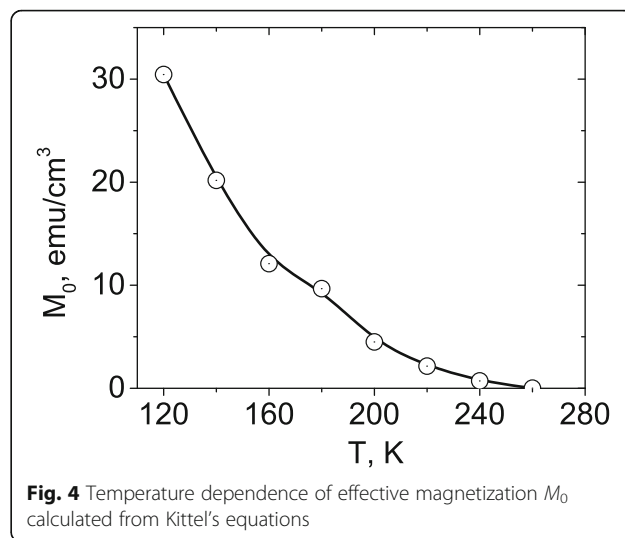
$$(\omega/\gamma)^2 = H_{\text{res}}^{\parallel} (H_{\text{res}}^{\parallel} + 4\pi M_0) \tag{1}$$

$$\omega/\gamma = H_{\text{res}}^{\perp} - 4\pi M_0 \tag{2}$$

where $H_{\text{res}}^{\parallel}$ and H_{res}^{\perp} are, respectively, the resonance fields for H parallel and perpendicular to the film plane, ω is angular frequency, and γ is gyromagnetic ratio.

Figure 4 shows temperature dependence of the effective magnetization M_0 obtained by the solution of the system of Eqs. (1)–(2) with the use of experimental resonance fields $H_{\text{res}}^{\parallel}$ and H_{res}^{\perp} . It is seen that M_0 decreases from 30 emu/cm³ to zero as temperature rises from 120 to 260 K. At temperatures higher than 260 K, the sample is in PM state.

It should be noted that bulk LBMO displays FM to PM transition near 340 K [2, 5]. The reduced Curie temperature in the LBMO/ZnO nanostructure may be



caused by relatively strong lattice mismatch between LBMO and ZnO [22].

Taking into account the complexity of the ESR spectra and non-negligible background noise, additional measurements were made to prove the reliability of the obtained results. Detailed angle dependences of the ESR spectra may provide additional important information about magnetic state of a complex system. Such studies were carried out for the LBMO/ZnO nanostructure at $T = 160$ K. Figure 5 shows the spectra obtained for different values of the angle θ between external magnetic field H and film normal. Here again, we see relatively intensive absorption line whose resonance field does not depend on θ (signal from PM phase) and the line of weaker intensity, whose position changes as the sample is rotated (signal from FM phase).

The spectra were analyzed by fitting to the sum of the derivatives of Lorentzians [28]:

$$\frac{dP}{dH} \propto \frac{d}{dH} \left\{ \frac{\Delta H_1}{(H - H_{\text{res}1})^2 + \Delta H_1^2} \right\} + \frac{d}{dH} \left\{ \frac{\Delta H_2}{(H - H_{\text{res}2})^2 + \Delta H_2^2} \right\} \tag{3}$$

where H_{resi} and ΔH_i ($i = 1, 2$) are, respectively, resonance field and width of the corresponding line. The results of the fitting are shown in Fig. 5 by solid lines.

Figure 6 shows the angle dependence of the resonance field $H_{\text{res}2}$ for FM phase (circles). To analyze the $H_{\text{res}2}$ vs θ dependence, one should go beyond the Kittel's equations. In general, the resonance conditions for a FM system are governed by the behavior of the density of free energy E and can be found from the equation [29]:

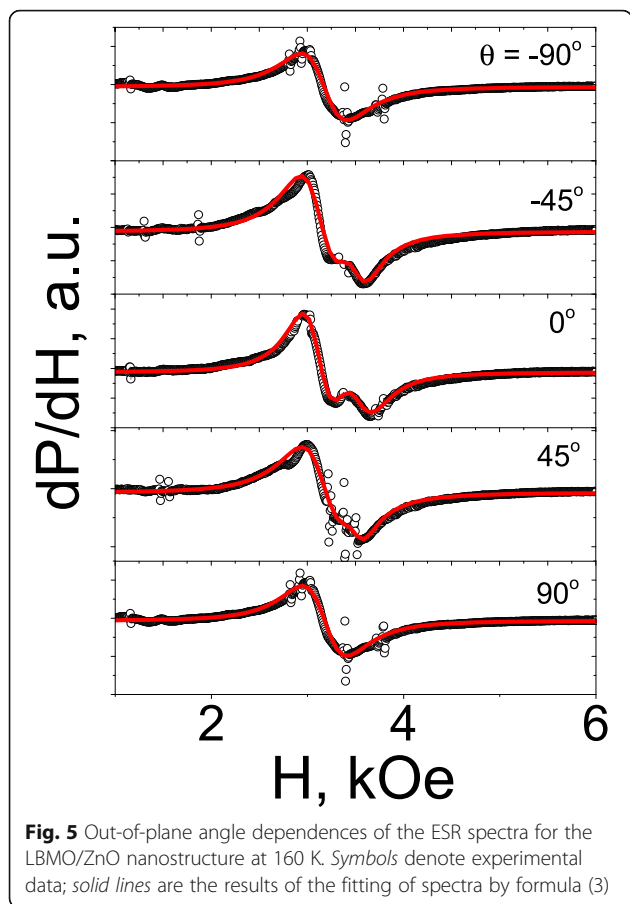


Fig. 5 Out-of-plane angle dependences of the ESR spectra for the LBMO/ZnO nanostructure at 160 K. Symbols denote experimental data; solid lines are the results of the fitting of spectra by formula (3)

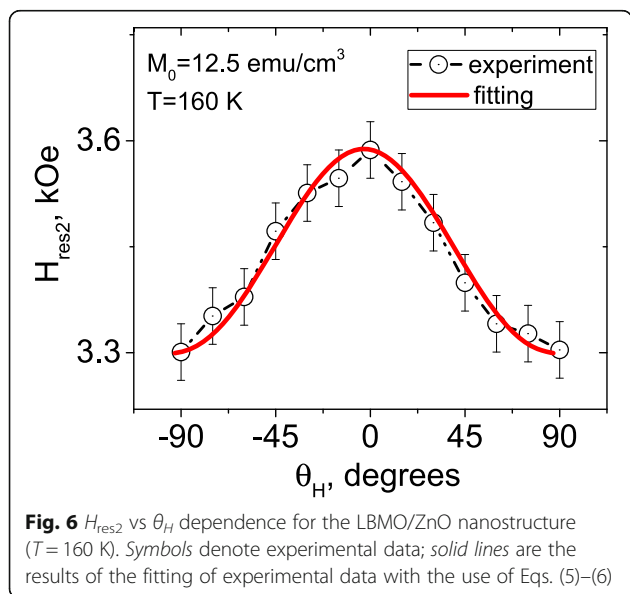


Fig. 6 H_{res2} vs θ_H dependence for the LBMO/ZnO nanostructure ($T = 160$ K). Symbols denote experimental data; solid lines are the results of the fitting of experimental data with the use of Eqs. (5)–(6)

$$\left(\frac{\omega}{\gamma}\right)^2 = \frac{1}{(M_0 \sin\theta_M)^2} (E_{\theta_M\theta_M} E_{\phi_M\phi_M} - E_{\theta_M\phi_M}^2) \quad (4)$$

where θ_M and ϕ_M are, respectively, polar and azimuthal coordinates of effective magnetization ($\mathbf{M} = (M_0, \theta_M, \phi_M)$), and E_{ij} ($i, j = \theta_M, \phi_M$) denote partial derivatives of E with respect to θ_M and ϕ_M variables. In the case of a thin FM film, the energy density is [30]:

$$E = -M_0 H [\sin\theta_H \sin\theta_M \cos(\phi_H - \phi_M) + \cos(\theta_H - \theta_M)] + 2\pi M_0^2 \quad (5)$$

where θ_H and ϕ_H are, respectively, polar and azimuthal coordinates of external magnetic field: $\mathbf{H} = (H, \theta_H, \phi_H)$.

An additional necessary condition for the resonance to be fulfilled is the minimization of the energy of FM sample with respect to the angles θ_M and ϕ_M :

$$\partial E / \partial \theta_M = 0, \quad \partial E / \partial \phi_M = 0 \quad (6)$$

In our case, since the measurements were carried out for $\phi_M = \text{const}$, only polar angles are remained in Eqs. (5)–(6).

After numerical solution of the system of Eqs. (5)–(6), the H_{res2} vs θ_H dependence was obtained, which is shown in Fig. 6 by solid line. Satisfactory agreement between the experimental and fitted data makes it possible to calculate the value of effective magnetization: $M_0 = 12.5 \text{ emu/cm}^3$. This value is close to that obtained earlier from Kittel’s equations $M_0 \text{ Kittel} \approx 12.1 \text{ emu/cm}^3$.

It was suggested in works [21, 22, 31] that the driving mechanism for resistive switching in the LBMO/ZnO nanostructures is a coexistence of highly conductive FM phase and poorly conducting charge-ordered phase in manganite layer. Our investigations confirm the existence of mixed magnetic state at temperatures lower than 260 K. At the same time, they show that at temperatures higher than 260 K, the manganite layer is paramagnetic. This, however, does not ultimately exclude the magnetic phase separation as possible driving mechanism for resistive switching at temperatures exceeding 260 K. There is a possibility of the existence of tiny amount of FM phase above 260 K which cannot be detected by the present ESR analysis. This phase could form very thin percolating paths which could be easily disconnected by the current heating, causing the switching from lower to higher resistance state.

Other possible driving mechanism for resistive switching, namely temperature-enhanced electric-field-induced migration of oxygen vacancies, was suggested in Ref. [32] for nanoscale manganite structures. The authors of this work use combination of electric fields and Joule self-heating to change the oxygen stoichiometry and promote oxygen vacancy drift in a free-standing $\text{La}_{0.7}\text{Sr}_{0.3}\text{MnO}_3$

thin film microbridge placed in controlled atmosphere. By controlling the local oxygen vacancies concentration, the LSMO-based microbridges were reversibly switched from metallic to insulating behavior on timescales lower than 1 s and with small applied voltages (<5 V). Multiple resistive states were shown to be set by selected current pulses which determined different oxygen vacancy profiles within the device.

Conclusions

Structure, electric, and resonance properties of LBMO/ZnO nanostructure fabricated on SrTiO₃ (001) substrate by ion-beam sputtering have been studied in this work. The layer thickness is near 100 nm for each of two layers. X-ray diffraction studies show that the main orientation of ZnO is (001), and LBMO has single phase of (110).

The LBMO/ZnO nanostructure shows fine rectification behavior at room temperature (295 K), and for relatively low voltage ($|V| < 0.2$ V), the I - V characteristics are fully reversible. At the same time, resistive switching is observed after application of higher voltages.

ESR measurements have been carried out in the temperature range from 120 to 300 K. It is demonstrated that nucleation of ferromagnetic phase occurs at 260 K and magnetic state below this temperature is characterized by coexistence of ferromagnetic and paramagnetic phases. As temperature decreases below 260 K, the effective magnetization of ferromagnetic phase increases and reaches 30 emu/cm³ at 120 K. No evidence of magnetic phase separation is found that at temperatures higher than 260 K.

Possible driving mechanisms for resistive switching have been discussed. It is concluded that magnetic phase separation and/or electric field-induced migration of oxygen vacancies, may be operative in the sample under investigation.

Acknowledgements

The work is partly supported by the Ministry of Education and Science of Ukraine through Indo-Ukraine International project "Spectroscopy study of multifunctional multiferroics materials" (Protocol MES of Ukraine from 09.09.2015). Dr. G.S. Lotey gratefully acknowledges the Department of Science and Technology (DST), Government of India, for providing funding, to carry out this research work under Indo-Ukraine International project via their sanction letter no. INT/UKR/P-17/2015 dated 14 August 2015. The authors are thankful to Dr. V. Golub for fruitful discussions and assistance with ESR measurements.

Authors' Contributions

TE fabricated LBMO/ZnO nanostructures. TE and YN studied current-voltage characteristics. MS carried out X-ray investigations. TP performed temperature-dependent measurements of ESR spectra. GL and AT analyzed the results of ESR investigations. All authors contributed to analysis of experimental data and writing manuscript. AT supervised the work and finalized the manuscript. All authors read and approved the final manuscript. All authors have the appropriate permissions and rights to the reported data. All authors have agreed to the authorship and order of authorship.

Competing Interest

The authors declare that they have no competing interests.

Author details

- ¹Institute of Magnetism, 36b Vernadsky Boulevard, Kyiv 03680, Ukraine. ²Department of Physics, Taras Shevchenko National University of Kyiv, Volodymyrska Street, 64/13, Kyiv 01601, Ukraine. ³Sagamihara Surface Lab, 1880-2 Kamimizo, Chuoku, Sagamihara, Kanagawa 252-0243, Japan. ⁴University of Tokyo, 7 Chome-3-1 Hongo, Bunkyo, Tokyo, Japan. ⁵Department of Physics, Nano Research Lab, DAV University, Jalandhar, Punjab 144012, India.

Received: 29 December 2016 Accepted: 27 February 2017

Published online: 09 March 2017

References

- Bednorz JG, Müller KA (1993) Possible High T_c Superconductivity in the Ba-La-Cu-O System. In: Ott HR (ed) Ten years of superconductivity: 1980-1990, vol 7. Springer Netherlands, Dordrecht, pp 267-271
- Dagotto E, Hotta T, Moreo A (2001) Colossal magnetoresistant materials: the key role of phase separation. *Phys Rep* 344(1-3):1-153. doi:10.1016/S0370-1573(00)00121-6
- Khodzitsky MK, Kalmykova TV, Tarapov SI et al (2009) Left-handed behavior of strontium-doped lanthanum manganite in the millimeter waveband. *Appl Phys Lett* 95(8):082903. doi:10.1063/1.3204004
- Khodzitsky MK, Tarapov SI, Belozorov DP et al (2010) Negative permittivity and left-handed behavior of doped manganites in millimeter waveband. *Appl Phys Lett* 97(13):131912. doi:10.1063/1.3491155
- Dörr K (2006) Ferromagnetic manganites: spin-polarized conduction versus competing interactions. *J Phys D Appl Phys* 39(7):R125-R150. doi:10.1088/0022-3727/39/7/R01
- Endo T, Uehara K, Yoshii T et al (2010) Peculiar electrical and magnetic properties of La(Ba)MnO₃ thin films. *Trans Mat Res Soc Japan* 35(4):727-738. doi:10.14723/tmrsj.35.727
- Dolgin B, Belogolovskii M, Wu XD et al (2012) Metastable resistivity states and conductivity fluctuations in low-doped La_{1-x}Ca_xMnO₃ manganite single crystals. *J Appl Phys* 112(11):113907. doi:10.1063/1.4768264
- Tang ZK, Wong GKL, Yu P et al (1998) Room-temperature ultraviolet laser emission from self-assembled ZnO microcrystallite thin films. *Appl Phys Lett* 72(25):3270. doi:10.1063/1.121620
- Lee J, Hong B, Park YS (2013) Characteristics of sputtered ZnO films for buffer layer in inverted organic solar cells. *Thin Solid Films* 547:3-8. doi:10.1016/j.tsf.2013.06.045
- Kang Y, Lim K, Jung S et al (2012) Spray-coated ZnO electron transport layer for air-stable inverted organic solar cells. *Sol Energy Mater Sol Cells* 96:137-140. doi:10.1016/j.solmat.2011.09.045
- Jouane Y, Collis S, Schmerber G et al (2013) Influence of flexible substrates on inverted organic solar cells using sputtered ZnO as cathode interfacial layer. *Org Electron* 14(7):1861-1868. doi:10.1016/j.orgel.2013.04.024
- Nakamura T, Homma K, Tachibana K (2013) Thin film deposition of metal oxides in resistance switching devices: electrode material dependence of resistance switching in manganite films. *Nanoscale Res Lett* 8(1):76. doi:10.1186/1556-276X-8-76
- Fujiwara K, Nemoto T, Rozenberg MJ et al (2008) Resistance switching and formation of a conductive bridge in metal/binary oxide/metal structure for memory devices. *Jpn J Appl Phys* 47(8):6266-6271. doi:10.1143/JJAP.47.6266
- Sawa A (2008) Resistive switching in transition metal oxides. *Mater Today* 11(6):28-36. doi:10.1016/S1369-7021(08)70119-6
- Zhang Z, Sun Y, Zhao Y et al (2008) Manganite thin film/ZnO nanowire (nanosheets) p - n junctions. *Appl Phys Lett* 92(10):103113. doi:10.1063/1.2896307
- Khachar U, Solanki PS, Choudhary RJ et al (2012) Current-voltage characteristics of PLD grown manganite based ZnO/La_{0.5}Pr_{0.2}Sr_{0.3}MnO₃/SrNb_{0.002}Ti_{0.998}O₃ thin film heterostructure. *Solid State Commun* 152(1):34-37. doi:10.1016/j.ssc.2011.10.013
- Ren R (2012) Spin polarization transport in ZnO/La_{2/3}Sr_{1/3}MnO₃/LaAlO₃ heterostructures. *J Phys Conf Ser* 400(1):12061. doi:10.1088/1742-6596/400/1/012061
- Feng Y, Zhang M (2010) Effects of ZnO film thickness on electrical and magnetoresistance characteristics of La_{0.8}Sr_{0.2}MnO₃/ZnO heterostructures. *J Magn Magn Mater* 322(18):2675-2679. doi:10.1016/j.jmmm.2010.04.006
- Liang Y (2011) Growth and structural characteristics of perovskite-wurtzite oxide ceramics thin films. *Ceram Int* 37(3):791-796. doi:10.1016/j.ceramint.2010.10.028

20. Lord K, Hunter D, Williams TM et al (2006) Photocarrier injection effect and p-n junction characteristics of $\text{La}_{0.7}\text{Sr}_{0.3}\text{MnO}_3$ / ZnO and Si heterostructures. *Appl Phys Lett* 89(5):052116. doi:10.1063/1.2335406
21. Yamada M, Sakai O, Nakamura T (2014) Spectroscopic ellipsometry analysis of perovskite manganite films for resistance switching devices. *Thin Solid Films* 571:597–600. doi:10.1016/j.tsf.2013.11.145
22. Okada A, Uehara K, Yokura M et al (2014) Double-layer fabrication of cubic-manganites/hexagonal-ZnO on various substrates by ion beam sputtering, and variable electrical property. *Jpn J Appl Phys* 53(5S1):05FB10. doi:10.7567/JJAP.53.05FB10
23. Tovstolytkin AI, Pogorily AM, Dzhezheriya YI et al (2009) Interference of coexisting para- and ferromagnetic phases in partially crystallized films of doped manganites. *J Phys Condens Matter* 21(38):386003. doi:10.1088/0953-8984/21/38/386003
24. Tovstolytkin AI, Dzyublyuk VV, Podyalovskii DI et al (2011) Complex phase separation in $\text{La}_{0.6}\text{Ca}_{0.4}\text{MnO}_3$ films revealed by electron spin resonance. *Phys Rev B* 83:18. doi:10.1103/PhysRevB.83.184404
25. Thiele C, Dörr K, Fähler S et al (2005) Voltage-controlled epitaxial strain in $\text{La}_{0.7}\text{Sr}_{0.3}\text{MnO}_3$ / $\text{Pb}(\text{Mg}_{1/3}\text{Nb}_{2/3})\text{O}_3$ - PbTiO_3 (001) films. *Appl Phys Lett* 87(26):262502. doi:10.1063/1.2150273
26. Tovstolytkin AI, Polek TI, Pod'yalovskii DI et al (2015) Electron spin resonance in ceramic samples of lanthanum—bismuth manganite $\text{La}_{0.925}\text{Bi}_{0.075}\text{MnO}_3$. *Metallofiz. Noveishie Tekhnol* 37(11):1503–1516. doi:10.15407/mfint.37.11.1503
27. Kittel C (1948) On the theory of ferromagnetic resonance absorption. *Phys Rev* 73(2):155–161. doi:10.1103/PhysRev.73.155
28. Celinski Z, Urquhart KB, Heinrich B (1997) Using ferromagnetic resonance to measure the magnetic moments of ultrathin films. *J Magn Magn Mater* 166(1-2):6–26. doi:10.1016/S0304-8853(96)00428-3
29. Suhl H (1955) Ferromagnetic resonance in nickel ferrite between one and two kilomegacycles. *Phys Rev* 97(2):555–557. doi:10.1103/PhysRev.97.555.2
30. Mizukami S, Ando Y, Miyazaki T (2001) The study on ferromagnetic resonance linewidth for NM/80NiFe/NM (NM = Cu, Ta, Pd and Pt) films. *Jpn J Appl Phys* 40(2R):580. doi:10.1143/JJAP.40.580
31. Mori T, Yokura M, Matsui M et al (2015) Evolution of I-V characteristics and photo effects of heterojunction LBMN/ZnO prepared by IBS. *Solid State Phenom* 230:19–27. doi:10.4028/www.scientific.net/SSP.230.19
32. Manca N, Pellegrino L, and Marre D (2017) Reversible oxygen vacancies doping in $(\text{La}_{0.7}\text{Sr}_{0.3})\text{MnO}_3$ microbridges by combined self-heating and electromigration. arXiv:1702.00826v1. doi: http://dx.doi.org/10.1063/1.4921342

Submit your manuscript to a SpringerOpen[®] journal and benefit from:

- Convenient online submission
- Rigorous peer review
- Immediate publication on acceptance
- Open access: articles freely available online
- High visibility within the field
- Retaining the copyright to your article

Submit your next manuscript at ► springeropen.com
